

***The peculiar behavior of the glass transition temperature of amorphous drug-polymer films coated on inert sugar spheres***

**Aswin Dereymaker<sup>1</sup> and Guy Van den Mooter<sup>1</sup>**

<sup>1</sup>Drug Delivery and Disposition, KU Leuven, Campus Gasthuisberg O&N2, Herestraat 49, Box 921, 3000 Leuven, Belgium

**Corresponding author:** Guy Van den Mooter – [guy.vandenmooter@pharm.kuleuven.be](mailto:guy.vandenmooter@pharm.kuleuven.be)

Address: Drug Delivery & Disposition, Campus Gasthuisberg O&N 2, Box 921, Herestraat 49, 3000 Leuven, Belgium. Tel.: +32 16 330304; fax: +32 16 330305

## **ABSTRACT**

Fluid bed coating has been proposed in the past as an alternative technology for manufacturing of drug-polymer amorphous solid dispersions, or so-called glass solution. It has the advantage of being a one step process, and thus omitting separate drying steps, addition of excipients or manipulation of the dosage form. In search of an adequate sample preparation method for mDSC analysis of beads coated with glass solutions, glass transition broadening and decrease of the glass transition temperature was observed with increasing particle size of crushed coated beads and crushed isolated films of indomethacin and polyvinylpyrrolidone. Substituting indomethacin with naproxen gave comparable results. When ketoconazole was probed or the solvent in INDO-PVP films was switched to DCM or a methanol-DCM mixture, two distinct T<sub>g</sub> regions were observed. Small particle sizes had a glass transition in the high T<sub>g</sub> region, large particle sizes in the low T<sub>g</sub> region. This particle size dependent glass transition was ascribed to different residual solvent amounts in the bulk and at the surface of the particles. A correlation was observed between the deviation of the glass transition temperature from that calculated from the Gordon-Taylor equation and the amount of residual solvent at the glass transition temperature of particles with different sizes.

Keywords: Amorphous, Glass transition, Solid dispersion, Thermal analysis, Thermogravimetric analysis, Modulated differential scanning calorimetry, Residual solvent, Fluid bed coating, Rotary evaporation, Bead coating

**List of abbreviations:**

API: active pharmaceutical ingredient

DCM: dichloromethane

DSC: differential scanning calorimetry

INDO: indomethacin

KETO: ketoconazole

mDSC: modulated differential scanning calorimetry

NAP: naproxen

PVP: polyvinylpyrrolidone

stdev: standard deviation

Tg: glass transition temperature

## 1. INTRODUCTION

Solid dispersions are considered to be one of the promising formulation strategies to increase the solubility and bioavailability of poorly soluble active pharmaceutical ingredients (API).<sup>1</sup> Despite being reported for the first time over 40 years ago<sup>2</sup>, only a limited number of approved drug formulations are on the market today.<sup>3</sup> While there are many subdivisions of solid dispersions, attention nowadays is focused on glass solutions where the drug is molecularly dispersed into an amorphous carrier (mostly polymers), resulting in a one phase system.<sup>4,5</sup> Because solid dispersion manufacturing often leads to supersaturated glass solutions which are in thermodynamical non-equilibrium, risks of phase separation into drug rich and polymer rich regions are constantly present, which can ultimately lead to crystallization of the API and the subsequent loss of its solubility advantage.<sup>6</sup> Phase separation risk can even be increased by absorption or adsorption of water from the environment, residual solvent or manipulations of the glass solutions into final dosage forms.

In addition to spray drying as a well-established manufacturing procedure for glass solutions via the solvent method, fluid bed coating can be proposed as a viable alternative. As compared to spray drying, fluid bed coating is a largely unexplored manufacturing method and has numerous potential advantages. It allows the formulation to be dried immediately into the coating device. This is very important to remove residual solvents from the system, because these are often toxic and can cause unwanted plasticization of the system. Also, the coating of beads omits any additional processing steps, like milling or compression, to acquire a final dosage form. These additional processing steps have

been shown to lead to solid state changes, for example compression which induced amorphous-amorphous phase separation in spray dried solid dispersions.<sup>7</sup>

Few studies have been previously reported in literature, mostly emphasizing on the solubility advantage of the solid dispersions prepared by coating in comparison with the pure drug substance. However, a thorough understanding of the physical structure and phase behavior is of the utmost importance for the estimation of the stability of the produced solid dispersions. To analyze this phase behavior, differential scanning calorimetry (DSC) is one of the tools of choice. It is able to detect the most important markers of instability in solid dispersions, namely amorphous-amorphous phase separation, enthalpic recovery of amorphous materials and the presence of crystalline API. Due to solid dispersions being multi-component systems and the production method, some transitions can overlap in a standard DSC. In modulated differential scanning calorimetry (mDSC), where the total heat flow can be mathematically separated (a deconvolution operation) into a reversing heat flow (a measure of the sample's heat capacity) and a non-reversing heat flow signal (heat flow associated with kinetic or kinetically controlled processes), these overlapping transitions can be clearly distinguished. For example, when preparing solid dispersions using the solvent evaporation method, some residual solvent can remain present in the system, upon evaporation due to heating in the DSC. This will be visible in the thermogram as a broad endotherm masking all other thermal events (glass transition). Due to the kinetic nature of solvent evaporation, this will be explicitly visible into the non-reversing heat flow signal in mDSC, provided a well optimized modulation program.

When glass solutions are produced, they are monophasic systems which will show one single glass transition, showing full miscibility of polymer and API. One of the most commonly used ways to calculate this mix-T<sub>g</sub> is by using the Gordon-Taylor equation<sup>8</sup>:

$$T_g = \frac{w_1 T_{g1} + k_{GT}(1-w_1)T_{g2}}{w_1 + k_{GT}(1-w_1)} \quad (\text{equation 1})$$

In this equation:  $T_{g1} \leq T_{g2}$  so  $T_{g1}$  usually represents the glass transition of the drug and  $T_{g2}$  the glass transition of the polymer.  $w$  is the weight fraction and the constant  $k_{GT} = \frac{\rho_1 \Delta\alpha_1}{\rho_2 \Delta\alpha_2} \approx \frac{\rho_1 T_{g1}}{\rho_2 T_{g2}}$ <sup>9</sup>, where  $\rho$  is the density of the component and  $\Delta\alpha$  the change in thermal expansivity of the component at  $T_g$ .<sup>10</sup>

In previously performed studies involving coated solid dispersions onto inert carriers, a lot of variation is seen in methodology of DSC/mDSC analysis. Hsiu-O et al.<sup>11</sup> and Zhang et al.<sup>12</sup> performed DSC analysis with the coated pellets loaded as such into the aluminium pans. Sun et al. did not analyze the produced solid dispersions with DSC.<sup>13</sup> In the study of Li et al. solid dispersion samples were prepared by spraying into the drying chamber without sugar pellets under the same coating conditions, and then the solid dispersions were peeled off carefully and ground to a fine powder for DSC analysis.<sup>14</sup> Nikowitz et al. did not specify any DSC sample preparation method in their paper about the study of recrystallization in coated pellets.<sup>15</sup> Lastly, in a recent study of Mahmoudi et al. amorphous solid drug dispersions were prepared via either rotary evaporation or fluid bed drug layering. Only powder samples from the rotary evaporation were analyzed by DSC.<sup>16</sup>

The aim of this study is to develop a reliable mDSC method for glass solutions, coated on an inert carrier, and the investigation of an interesting glass transition phenomenon associated with this method development.

Naproxen (NAP), indomethacin (INDO) and ketoconazole (KETO) were used as model drugs. Polyvinylpyrrolidone (PVP) K25 was selected as a model hydrophilic polymer. NAP and INDO both have hydrogen donors which can form hydrogen bonds with PVP, whereas KETO is unable to form hydrogen bonds with the polymer. NAP-PVP and INDO-PVP are well known solid dispersion systems which have been extensively studied in the past.<sup>17-21</sup>

## **2. MATERIALS AND METHODS**

### *2.1 Materials*

Naproxen and Indomethacin were purchased from FAGRON Ltd. (Waregem, Belgium), ketoconazole was a kind gift from Janssen Pharmaceutica (Beerse, Belgium), polyvinylpyrrolidone K 25 was a generous gift from BASF (Ludwigshafen, Germany). Sugar spheres (diameter 710 - 850  $\mu\text{m}$ ) were kindly donated by Hanns G. Werner GmbH (Tornesch, Germany).

### *2.2 Methods*

#### **2.2.1 Fluidized bed coating**

A 30-70% IND-PVP (1:2 weight ratio to beads) glass solution was coated onto 500g of beads from a 6.67% (w/v) ethanol solution, using bottom spray fluid bed coating.

The sugar spheres were loaded into the preheated coating chamber of an Aeromatic MP 1 multiprocessor (GEA, Switzerland). The sugar beads were heated for half an hour. The drug-polymer solution was coated onto the sugar beads using a bottom spray set-up with a Würster insert. When the spraying was finished, the pellets were dried until immobilization due to electrostatic charges. The coated spheres were unloaded, weighed and dried for an additional 48 hours in an oven at 40°C.

In the formation of the INDO-PVP beads, the air volume was set at 1566.3L/min, inlet temperature was 50°C, atomizing air pressure 1.5 bar and the feed rate was 6 ml/min.

After 48 hours of drying in a hot air oven at 40°C, sugar beads were crushed with a pestle in a mortar and sieved into different particle size ranges.

#### **2.2.2 Film formation by rotary evaporation**

Glass solution films were made using a Büchi Rotavapor R-210 (Flawil, Switzerland). API-polymer (30-70% w-w) was dissolved into a common solvent (ethanol, Dichloromethane (DCM) or a 1:1 (v/v) mixture of DCM and methanol) to form a 10% (w/v) solution. The water bath was set to 60°C for ethanol solutions and 40°C for DCM and DCM-methanol solutions. A round bottom flask with the solution was rotated into the water bath under vacuum. After formation of a film, the glass solution was dried for an additional 48 hours in an oven at 40°C. In accordance with the coated beads, the films were crushed and sieved in different particle size ranges for analysis.

### **2.2.3 Modulated temperature differential scanning calorimetry (mDSC)**

mDSC measurements were carried out with a TA instruments Q2000 modulated DSC (Leatherhead, UK) equipped with a refrigerated cooling system (RCS90). During analysis, the DSC cell was purged with a nitrogen flow of 50 ml/min. Mathematical analysis of the data was performed using TA Instruments Universal Analysis software (version 4.4, Leatherhead, UK). TA Instruments standard aluminium pans (Brussels, Belgium) were used for all measurements. Glass transition temperatures were measured at half height in the reversing heat flow. The step jump in heat capacity observed in the reversing heat flow signal was further examined in the corresponding derivative signal after Savitsky-Golay smoothing with points of window set at 20. The first derivative of the reversing heat flow was chosen to visualize the glass transitions because discrete changes are much better visible in the peaks of the derivative reversing heat flow, as compared with the small baseline shifts of the original reversing heat flow.

Octadecane and indium were used to calibrate the DSC temperature scale, the enthalpic response was calibrated with indium. The heat capacity was calibrated using sapphire disks.

All sample masses were between 4-7 mg (accurately weighed). The samples were kept isothermal at 40°C for 60 minutes, followed by heating from 40°C to 180°C (or 0-200°C depending on the experiment) for the glass solution films and 0°C to 165°C for the coated beads. A heating rate of 2°C/min was applied with a temperature modulation of 0.636°C every 40s. All samples were measured in duplicate.

#### **2.2.4 Thermo gravimetric Analysis**

The prepared samples (coated beads and films, crushed and sieved) were analyzed using a TA instruments SDT Q600 (Leatherhead, UK) to determine moisture and volatile contents. The samples were heated at 5°C/min from 25 °C to 150 °C in a continuous mode in a first type of experiment. In the second type of experiment, samples were kept isothermal at 50°C for 20 hours, heated to 140°C at 10°C/min and kept isothermal for 2 hours, and finally cooled again to 50°C at 10°C/min and kept isothermal for 1 hour. Finally, in a third experiment samples were kept isothermal at 40°C for 1 hour and subsequently heated at 2°C per minute to 170°C. A dry N<sub>2</sub> purge of 100 mL/min was used to be able to maintain an inert environment. Weight loss due to solvent and moisture evaporation was calculated as percentage weight loss compared to the original sample mass. Sample masses are between 10 and 20 mg (accurately weighed).

### 3. RESULTS AND DISCUSSION

#### *3.1 mDSC analysis of INDO-PVP (30/70% w/w) glass solutions, coated onto sugar beads*

As mentioned above, no universally applicable sample preparation method exists for the DSC analysis of coated beads. In search of effective sample preparation for mDSC analysis, the bottom of a DSC pan was filled with coated beads and analyzed. This approach produced no visible signal other than the melting peak of sucrose. It was clear that the contact area between the coating and the bottom of the pan was insufficient. In a second attempt, beads were crushed to improve thermal contact. However, the only visible transition was the melting of the sucrose beads, leading to the observation that there was, proportionally, too much sucrose present. In a next step, beads were crushed gently with a pestle and mortar and sieved to separate different particle sizes in an attempt to find a specific particle size range where more coating was present relative to the sucrose content. This sieving was performed using seven sieves (pore diameter: 32 $\mu$ m, 63 $\mu$ m, 90 $\mu$ m, 150 $\mu$ m, 250 $\mu$ m and 355 $\mu$ m). After sieving for an adequate time the material on top was discarded (larger than 355 $\mu$ m), the other material was collected and stored separately for each particle size range. Subsequently, six different particle size ranges were stored in closed containers: 0-32 $\mu$ m, 32-63 $\mu$ m, 63-90 $\mu$ m, 90-150 $\mu$ m, 150-250 $\mu$ m and 250-355 $\mu$ m. Figure 1 shows the first derivate of the reversing heat flow in function of temperature for the different particle sizes of crushed and sieved INDO-PVP beads.

Surprisingly, the data show a shift and broadening of the glass transition region with increasing particle size. Table 1 lists the numerical values of the mean glass transition onset, offset, range and half-height temperature of 3 replicate experiments.

There is a difference of 26.2°C between mean glass transition temperature of the smallest and largest particle size range. The glass transition range has also increased with ca. 18°C, which means the mean width has become more than doubled, hence a large broadening of the glass transition region.

This glass transition shift is probably also the reason why it only becomes visible in DSC after sieving. When the beads are only crushed, there is a large particle size variety present, so the sample will have multiple small glass transitions which will lead to a very broad signal in the reversing heat flow, which is not detectable by mDSC.

### *3.2 mDSC analysis of INDO-PVP (30/70% w/w) glass solution films*

To confirm this particle size induced glass transition temperature decrease and broadening in a more simple formulation, INDO-PVP films were made by rotary evaporation. In essence, this is the way the glass solutions are formed on the sucrose beads during fluid bed coating. Droplets form miniature films around the inert carrier and are dried during cycling in the fluidized bed. When reentering the Würster insert and being sprayed upon, this process repeats itself. Derivative reversing heat flow signals in function of temperature for the different particle size ranges are shown in Figure 2 for a first and second heating cycle. After the first heating cycle is completed, the sample is cooled at maximum capacity of the Q2000 DSC (around 30°C/min). After temperature equilibration at 0°C the second heating cycle is initiated with the same heating rate and modulation parameters used during first heating.

All numerical information about the glass transition is given in Table 2. From the INDO-PVP films, it's also evident that T<sub>g</sub> shifts to lower temperatures and broadens as the particle size increases. There is an 18.4°C difference in temperature shift and a 16.6°C

broadening between the values of the smallest and largest particle size. These differences disappear respectively to 3.6°C and 1.9°C when the sample is cooled and reheated.

The dependence of the glass transition temperature on the particle size has, to the best of our knowledge, never been reported before. Contrary to the well-known melting point depression related to particle size reduction<sup>22</sup>, there is no fundamental physical phenomenon known to explain the dependence of the glass transition temperature on the particle size.<sup>21</sup> The trend observed in the coated beads was thus confirmed and even more pronounced in the glass solution films. Furthermore, when samples are cooled and reheated in the mDSC, all differences virtually disappear. These observations lead to two possible explanations. First, there can be a difference in mixing for different particle sizes. When a particle with a larger size would have a higher ratio of indomethacin compared to the particles with smaller size, the glass transition would be lower. This could be seen as different phases in different particle sizes. However, this would be highly unlikely because the films are prepared from a solution where drug and polymer are fully dissolved. It is evenly unlikely that these different drug-polymer ratios are induced while crushing the films or beads because the samples are crushed with the same intensity and during the same amount of time. A second hypothesis can be proposed where different particle sizes have different amounts of residual solvents, which can act as a plasticizer and thus cause a decrease in glass transition temperature of the system.

The heat-cool-heat experiment cannot exclude one of the hypotheses. Residual solvent will be completely removed when heating up to 180°C and plasticizing effects of these solvents will be eliminated when the sample is reheated. However heating above the glass transition also increases the mobility of the (amorphous) drug and polymer, which

can affect the mixing of drug and polymer, also eliminating the observed differences in the first heating step.

Previous studies provide the data to calculate the glass transition temperature of glass solutions with the Gordon-Taylor equation for this drug-polymer system. Glass transition temperature (430 K) and density (1.14 g/cm<sup>3</sup>) for PVP K25 are taken from Paudel et al.<sup>17</sup>, glass transition temperature (315 K) and density (1.31 g/cm<sup>3</sup>) of indomethacin from Matsumoto and Zograf<sup>21</sup>. Calculation yielded a glass transition temperature of the glass solution of 118°C. Glass transitions of the second heating cycles are closest to this ideal mixing T<sub>g</sub>. The reason is of course that in the second heating cycle most of the residual solvents (which act as plasticizer) are eliminated from the glass solutions and not that the system is approaching ideal behavior (as the values are close to those calculated from the Gordon-Taylor equation in the second heating cycle). When considering the first heating cycle, particles with the smallest size have a glass transition temperature closest to 118°C, which points out that at the glass transition, the smallest particles contain the least residual solvent.

Different observations were made when the same film fragments, divided in different size ranges, were stored at room temperature for 7 weeks and reanalyzed with mDSC. The thermograms of the different particle size ranges are shown in Figure 3. The observed glass transition shift observed in the initial thermogram, has now disappeared. Only the particles with the largest size still show a decrease in T<sub>g</sub>.

Storage at room temperature can enable the samples to further dry and get rid of the residual solvents, but storage at room temperature, which is far below the glass transition temperature of the glass solutions, does not provide the necessary mobility to

spontaneously induce mixing of the systems. It can be reasonably assumed that larger particles, which have a much smaller surface area to mass ratio, and thus contact surface with the surroundings (air), need a longer time to lose their residual solvent. This is the reason why the particles with the largest size range still have a decreased glass transition temperature. This experiment thus reinforces the residual solvent hypothesis.

### *3.3 mDSC analysis of glass solution films of Naproxen-PVP and Ketoconazole-PVP (30-70% w-w)*

In order to confirm the generality of the observed phenomenon, systems with a different API (Naproxen and Ketoconazole) were selected and compared with the same polymer and in the same ratio to solely investigate the influence of changing the active component. Ketoconazole was chosen because, contrary to INDO and NAP, it doesn't have any hydrogen donor groups and is thus unable to form hydrogen bonds with PVP. Figure 4 shows the derivative of the reversing heat flow for NAP-PVP (30-70% w/w) and KETO-PVP (30-70% w/w) in function of temperature for 5 different particle size ranges.

The different particle sizes for the NAP-PVP glass solution again show a distinct glass transition decrease for increasing particle size, although this decrease is mainly observed between the two smallest particle sizes, further decrease is more discrete. KETO-PVP shows a different pattern, as in these glass solution particles, two different glass transition regions can be distinguished. Particles with smaller sizes (0-32 $\mu$ m and 32-63 $\mu$ m) predominantly reside in the high T<sub>g</sub> region, around 115-120°C. Particles with larger sizes (150-250 $\mu$ m and 250-355 $\mu$ m) are mainly in the low T<sub>g</sub> region, around 60-70°C. The particles with an intermediate size range (between 63-90 $\mu$ m) have two T<sub>g</sub> peaks, one in each region.

While the NAP-PVP samples confirmed the trend observed with the INDO-PVP samples, KETO-PVP showed a slightly different behavior, though still a particle size dependent glass transition temperature.

For the calculation of the Gordon-Taylor equation, glass transition temperature (279K) and density (1.25 g/cm<sup>3</sup>) of naproxen are taken from Paudel et al.<sup>17</sup> and T<sub>g</sub> (317.5K) and density (1.30g/cm<sup>3</sup>) of ketoconazole from Van den Mooter et al.<sup>23</sup> Glass transition temperature for naproxen is calculated at 100°C and for ketoconazole at 119°C. It is again obvious that glass transitions from the smallest particles are closest to the calculated mixing T<sub>g</sub>, thus reinforcing again the role of the available surface area for solvent evaporation.

#### *3.4 mDSC analysis of INDO-PVP (30/70% w/w) glass solution films from a 10% (w/v) DCM and DCM-methanol (50-50% v-v) solution*

To investigate the influence of different solvents on the phase behavior and resulting glass transition decrease with particle size, ethanol as solvent was replaced by dichloromethane and a 1:1 mixture of dichloromethane and methanol. For the pure DCM 5 particle size ranges up to 250µm were tested, for the DCM-methanol mixture 7 particle size ranges were tested, up to 425µm. Figure 5 represents the derivative reversing heat flow in function of temperature for the different particle size ranges of DCM (A) and DCM-methanol (B).

With the change of solvent, the same phenomenon was observed as in the KETO-PVP glass solutions, produced from an ethanol solution. For DCM as well as DCM-methanol, a distinction can again be made between a high T<sub>g</sub> region with predominantly the particles with smaller size ranges on one hand, and a low T<sub>g</sub> region with the particles

with larger size ranges on the other hand. Intermediate particle size ranges again show a glass transition in the high T<sub>g</sub> region as well as in the low T<sub>g</sub> region. These experiments show the separation in T<sub>g</sub> regions is not a phenomenon that can be solely described to KETO-PVP, but something as simple as a change in solvent can induce this separation.

### *3.5 TGA analysis of INDO-PVP (30-70% w-w) glass solution films*

To be able to take into account the role of the residual solvent, present in the film particles, and/or the amount of absorbed water from the environment into the particles, TGA analysis was performed on all of the particle size ranges. Table 3 represents the average weight loss of different particle size ranges of INDO-PVP using a heating program of 5°C/min from 25°C to 150°C. These experiments clearly show a more or less equal amount of solvent in particles of a different size range. This seems to disprove the solvent hypothesis. However, a second TGA analysis was performed on 3 particle sizes of the INDO-PVP films, to differentiate between weight loss sub-T<sub>g</sub> (50°C) and above-T<sub>g</sub> (140°C). Figure 6 represents the weight (%) and temperature (°C) in function of time (min) for 0-32µm, 90-150µm and 250-355µm particles.

In the first isothermal step at 50°C, the smaller the particles, the more weight is lost due to evaporation of residual solvent, which can be explained by its higher surface area to mass ratio. Despite being dried for 20 hours, all particle size samples still contain residual solvent, which isn't released before heating above the glass transition temperature. After completion of the experiment, particles in the range between 90-150µm and 250-355µm have lost almost exactly the same mass, the 0-32µm particle size range is only slightly higher.

These findings lead to the conclusion that there is a difference in residual solvent amount, but specifications need to be made. The glass transition shift with increasing particle size range is a result of differences in sub-Tg residual solvent evaporation. Due to the much higher surface area to mass ratio of the small particle size ranges, residual solvent can evaporate to a higher extent than from the particles with larger size ranges, where more bulk solvent will be present. When looking at mDSC thermograms with two distinct Tg regions, the high Tg region can be represented by the glass transition of the solvent poor surface of the film particles and the low Tg region by the solvent 'rich' bulk of the film particles. Gradually shifting of the glass transition can be seen as a more discrete transition than separation into two distinct Tg regions. These differences can be achieved during heating in the DSC cell or during the isothermal step of 40°C for 1 hour, programmed before every run. The fact that this glass transition decrease has disappeared after 7 weeks also supports this hypothesis because here the residual solvent could have had enough time to evaporate, except in the largest particle size range where a Tg decrease is still visible. These findings can shine another light on DSC experiments of solid dispersions, prepared by solvent methods like for instance spray drying, which may contain a very broad range of particle sizes. When only DSC analysis is performed on particles with an intermediate particle size range (see Figures 4 and 5), two glass transitions may theoretically be observed and falsely interpreted as a phase separated system, which in reality really are particles with different solvent poor surface/solvent rich bulk ratios. The broadening and gradual shift of glass transitions has already been reported before.<sup>24</sup> In this article, this shift and broadening is a result of moisture sorption, which results in a depressed Tg in the outer layers of glassy maltodextrin particles. It can be

stated that this effect is in fact a similar phenomenon of what was observed in this article but in the opposite direction.

In an attempt to prove the residual solvent hypothesis, a third TGA experiment was performed where the heating method was equal to the mDSC method, namely an isothermal step at 40°C for 1 hour and subsequently a heating step of 2°C/min to 170°C. When simultaneously performing these TGA and mDSC experiments on a freshly prepared INDO-PVP (30-70% w/w) film (from a 10% ethanol solution w/v), which was crushed and separated into different particle size ranges, it was possible to determine the exact residual solvent amount at the glass transition temperature of the different size ranges. Glass transition temperatures were determined in the mDSC experiment. Previously, the glass transition temperature of INDO-PVP (30-70% w/w) had been calculated using the Gordon-Taylor equation and was 118°C. From this temperature, we can calculate the deviation for each particle size range. This is described in Table 4 together with the solvent loss from the glass transition temperature to 170°C for each particle size range. When the deviation from the Gordon-Taylor temperature is put in function of the solvent loss from T<sub>g</sub> to 170°C, a correlation can be found, this is represented in Figure 7. As can be seen from Figure 7, the correlation has a good fit ( $R^2=0.983$ ). This indicates that the glass transition temperature decrease with increasing particle size is a result of the presence of the amount of residual solvent at the glass transition temperature, and not of the total amount of residual solvent. The glass transition temperature decrease is not in correspondence with the total amount of residual solvent because of the different evaporation rates, due to the different surface area to mass ratio's, discussed in the previous TGA experiment. This evaporation is an imminent consequence

of the manner in which DSC measures the glass transition temperature, namely by heating up the sample. When performing (m)DSC analysis on glass solutions, prepared by the solvent method, caution is necessary when interpreting glass transitions from particles with wide particle size ranges.

#### 4. CONCLUSION

In search of a suitable mDSC sample preparation method for glass solutions of INDO-PVP, coated on inert carriers, an interesting phenomenon arised. When crushed and sieved into different particle size ranges, glass transitions of the coated beads shifted to lower temperatures and broadened with increasing particle size range. These findings were confirmed for INDO-PVP films prepared by rotary evaporation. Substituting indomethacin with naproxen gave comparable results. When the API was ketoconazole and the solvent in INDO-PVP films was switched to DCM or a methanol-DCM mixture, two distinct T<sub>g</sub> regions were observed. Small particle sizes had a glass transition in the high T<sub>g</sub> region, large particle sizes in the low T<sub>g</sub> region. TGA experiments showed that, while total mass loss due to residual solvent evaporation for all particle sizes are more or less the same, there is a distinct difference for sub T<sub>g</sub> and above T<sub>g</sub> mass loss, due to huge differences in surface area to mass ratio. Differences in glass transition for different particle size ranges can be ascribed to differences in solvent-free surface and solvent-rich bulk ratios. A correlation was found between the solvent loss from the glass transition temperature on and the deviation from the Gordon-Taylor derived glass transition temperature for the different particle size ranges. This further indicates that the glass transition decrease in glass solution particles with increasing particle size is due to the amount of residual solvent present at the glass transition temperature of the particles.

## REFERENCES

1. Serajuddin ATM 1999. Solid dispersion of poorly water-soluble drugs: early promises, subsequent problems, and recent breakthroughs. *J Pharm Sci* 88: 1058-1066.
2. Sekiguchi K, Obi N 1961. Studies on absorption of eutectic mixture. I. a comparison of the behavior of eutectic mixture of sulfathiazole and that of ordinary sulfathiazole in man. *Chem Pharm Bull* 9:866–872.
3. Huang Y, Dai WG 2014. Fundamental aspects of solid dispersion technology for poorly soluble drugs. *Acta Pharm Sin B* 4:18-25.
4. Chiou WL, Riegelman S 1971. Pharmaceutical applications of solid dispersion systems. *J Pharm Sci* 60:1281-1302.
5. Dhirendra K, Lewis S, Udupa N, Atin K 2009. Solid dispersions: a review. *Pak J Pharm Sci* 22:234-246.
6. Van den Mooter G 2012. The use of amorphous solid dispersions: a formulation strategy to overcome poor solubility and dissolution rate. *Drug Discov Today Technol* 9: e79–e85.
7. Ayenew Z, Paudel A, Van den Mooter G 2012. Can compression induce demixing in amorphous solid dispersions? A case study of naproxen-PVP K25. *Eur J Pharm Biopharm* 81: 207-213.
8. Gordon M, Taylor JS 1952. Ideal copolymers and the second-order transitions of synthetic rubbers. I. non-crystalline copolymers. *J Appl Chem* 2:493-500.

9. Simha R, Boyer RF 1962. On a general relation involving the glass temperature and coefficients of expansion of polymers. *J Chem Phys* 37:1003–1007.
10. Kalogeras IM 2011. A novel approach for analyzing glass-transition temperature vs. composition patterns: application to pharmaceutical compound+polymer systems. *Eur J Pharm Sci* 42:470–483.
11. Hsiu-O H, Huei-Lin S, Tsuimin T, Ming-Thau S 1996. The preparation and characterization of solid dispersions on pellets using a fluidized-bed system. *Int J Pharm* 139:223-229.
12. Zhang X, Sun N, Wu B, Lu Y, Guan T, Wu W 2008. Physical characterization of lansoprazole/PVP solid dispersion prepared by fluid-bed coating technique. *Powder Technol* 182:480-485.
13. Sun N, Wei X, Wu B, Chen J, Wu W 2008. Enhanced dissolution of silymarin/polyvinylpyrrolidone solid dispersion pellets prepared by a one-step fluid-bed coating technique. *Powder Technol* 182:72-80.
14. Li J, Liu P, Zhang WL, Yang JK, Fan YQ 2012. Novel Tanshinone II A ternary solid dispersion pellets by a single-step technique: in vitro and in vivo evaluation. *Eur J Pharm Biopharm* 80:426-432.
15. Nikowitz K, Pintye-Hodi K, Regdon Jr G 2013. Study of recrystallization in coated pellets – effect of coating on API crystallinity. *Eur J Pharm Sci* 48:563-571

16. Mahmoudi ZN, Upadhye SB, Ferrizzi D, Rajabi-Siahboomi AR 2014. In vitro characterization of a novel polymeric system for preparation of amorphous solid drug dispersions. *AAPS J* 16:685-697.
17. Paudel A, Van Humbeeck J, Van den Mooter G 2010. Theoretical and experimental investigation on the solid solubility and miscibility of naproxen in poly(vinylpyrrolidone). *Mol Pharm* 7:1133-1148.
18. Paudel A, Van den Mooter G 2012. Influence of solvent composition on the miscibility and physical stability of naproxen/PVP K25 solid dispersions prepared by cosolvent spray-drying. *Pharm Res* 29:251-270.
19. Paudel A, Loyson Y, Van den Mooter G 2013. An investigation into the effect of spray drying temperature and atomizing conditions on miscibility, physical stability, and performance of naproxen-PVP K25 solid dispersions. *J Pharm Sci* 102:1249-1267.
20. Taylor LS, Zografi G 1997. Spectroscopic characterization of interactions between PVP and indomethacin in amorphous molecular dispersions. *Pharm Res* 14:1691-1698.
21. Matsumoto T, Zografi G 1999. Physical properties of solid molecular dispersions of indomethacin with poly(vinylpyrrolidone) and poly(vinylpyrrolidone-co-vinylacetate) in relation to indomethacin crystallization. *Pharm Res* 16:1722-1728.
22. Xu Q, Sharp ID, Yuan CW, Yi DO, Liao CY, Glaeser AM, Minor AM, Beeman JW, Ridgeway MC, Kluth P, Ager JW 3rd, Chrzan DC, Haller EE 2006. Large melting point hysteresis of Ge nanocrystals embedded in SiO<sub>2</sub>. *Phys Rev Lett* 97:155701.

23. Van den Mooter G, Wuyts M, Blaton N, Busson R, Grobet P., Augustijns P, Kinget R, 2001. Physical stabilisation of amorphous ketoconazole in solid dispersions with polyvinylpyrrolidone K25. *Eur J Pharm Sci* 12:261–269.
24. van Sleuwen RM, Zhang S, Normand V 2012. Spatial glass transition temperature variations in polymer glass: application to a maltodextrin-water system. *Biomacromolecules* 13:787-797.

Table 1: Mean glass transition onset, offset, range and half-height temperature of different particle size ranges of INDO-PVP coatings onto sucrose beads (n=3).

<i>n=3</i>	<i>Glass transition temperature (°C)</i>				
<b>Particle size (µm)</b>	<b>Onset</b>	<b>Offset</b>	<b>Range</b>	<b>Half Height</b>	<b>St dev Half Height</b>
<b>0-32</b>	105,9	122,6	16,7	<b>114,2</b>	0,7
<b>32-63</b>	104,8	121,2	16,4	<b>113,0</b>	0,8
<b>63-90</b>	101,8	123,3	21,5	<b>112,4</b>	2,9
<b>90-150</b>	84,1	116,0	31,9	<b>100,0</b>	0,4
<b>150-250</b>	69,3	108,6	39,3	<b>89,1</b>	2,2
<b>250-355</b>	70,4	105,4	34,9	<b>88,0</b>	0,2

Table2: Mean glass transition onset, offset, range and half-height temperature of different particle size ranges of INDO-PVP films in first and second heating cycle (n=3).

<i>n=3</i>	<i>Glass transition temperature (°C)</i>				
<i>1st heating cycle</i>					
<b>Particle size (µm)</b>	<b>Onset</b>	<b>Offset</b>	<b>Range</b>	<b>Half Height</b>	<b>St dev Half Height</b>
<b>0-32</b>	104,0	118,7	14,7	<b>111,3</b>	0,1
<b>32-63</b>	101,6	119,6	18,0	<b>108,9</b>	1,0
<b>63-90</b>	94,4	116,3	21,8	<b>105,4</b>	0,6
<b>90-150</b>	87,3	113,8	26,5	<b>100,6</b>	0,3
<b>150-250</b>	77,2	108,5	31,3	<b>93,0</b>	0,6
<i>2nd heating cycle</i>					
<b>Particle size (µm)</b>	<b>Onset</b>	<b>Offset</b>	<b>Range</b>	<b>Half Height</b>	<b>St dev Half Height</b>
<b>0-32</b>	107,3	123,1	15,9	<b>115,2</b>	0,6
<b>32-63</b>	107,7	123,2	15,4	<b>115,5</b>	0,1
<b>63-90</b>	106,8	122,9	16,0	<b>114,8</b>	0,3
<b>90-150</b>	105,9	122,3	16,3	<b>114,0</b>	0,4
<b>150-250</b>	102,8	120,5	17,7	<b>111,6</b>	0,0

Table 3: weight loss (%) for different particle size ranges of INDO-PVP film

<i>INDO-PVP FILMS</i>	<b>sample 1</b>	<b>sample 2</b>	<b>MEAN</b>
<b>Particle size (µm)</b>	<b>Weight loss (%)</b>	<b>Weight loss (%)</b>	<b>Weight loss (%)</b>
<b>0-32</b>	3,877	4,793	<b>4,335</b>
<b>32-63</b>	4,488	4,280	<b>4,384</b>
<b>63-90</b>	4,565	4,431	<b>4,498</b>
<b>90-150</b>	3,983	4,157	<b>4,070</b>
<b>150-250</b>	4,690	4,220	<b>4,455</b>

Table 4: Weight loss from the glass transition temperature (%) and Gordon-Taylor Tg temperature depression (%) for the different particle size ranges of INDO-PVP film

<i>INDO-PVP FILM (30-70% w/w)</i>		
<b>Particle size (<math>\mu\text{m}</math>)</b>	<b>Solvent loss from Tg to 170°C (%)</b>	<b>Gordon-Taylor Tg temperature depression (%)</b>
<b>0-32</b>	1,35	95,29
<b>32-63</b>	1,86	87,40
<b>63-90</b>	2,21	84,54
<b>90-150</b>	2,51	78,07
<b>150-250</b>	2,74	77,65
<b>250-355</b>	3,15	70,77

Figure 1: Derivative reversing heat flow in function of temperature for different particle size ranges of crushed and sieved INDO-PVP (30/70% w/w) coated sucrose beads.

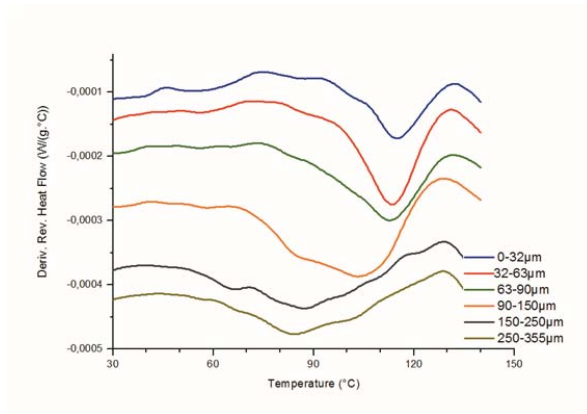


Figure 2: Derivative reversing heat flow in function of temperature for INDO-PVP films in the first 5 (A) and second (B) heating cycle for different particle sizes.

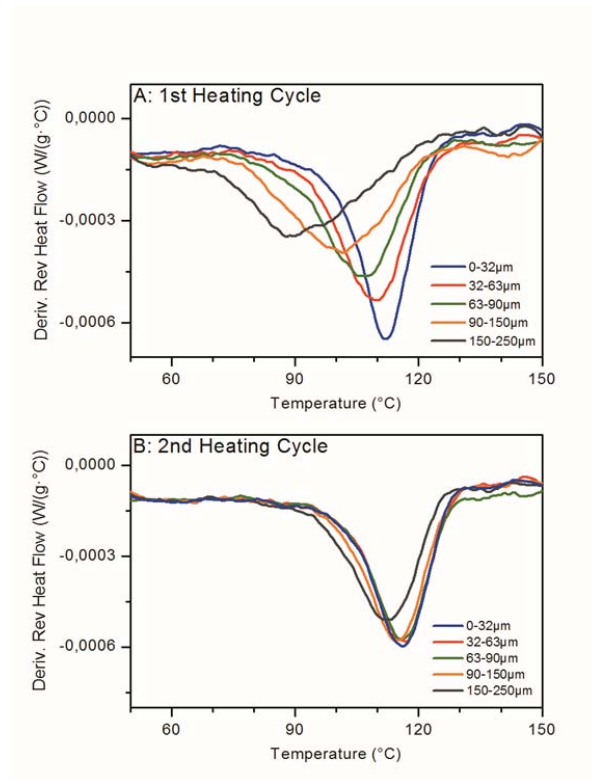


Figure 3: Derivative reversing heat flow in function of temperature for different particle size INDO-PVP films after storage at room temperature for 7 weeks.

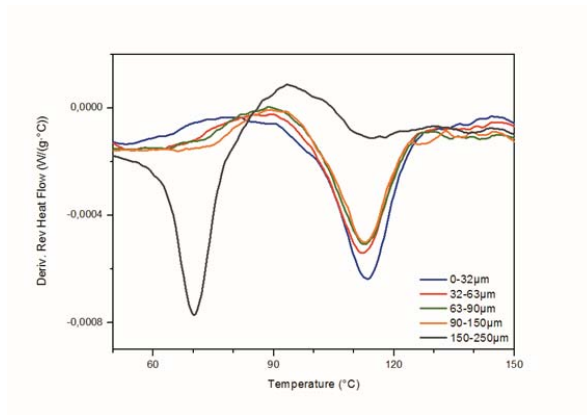


Figure 4: Derivative reversing heat flow thermogram of NAP-PVP (A) and KETO-PVP (B) for 5 different particle sizes.

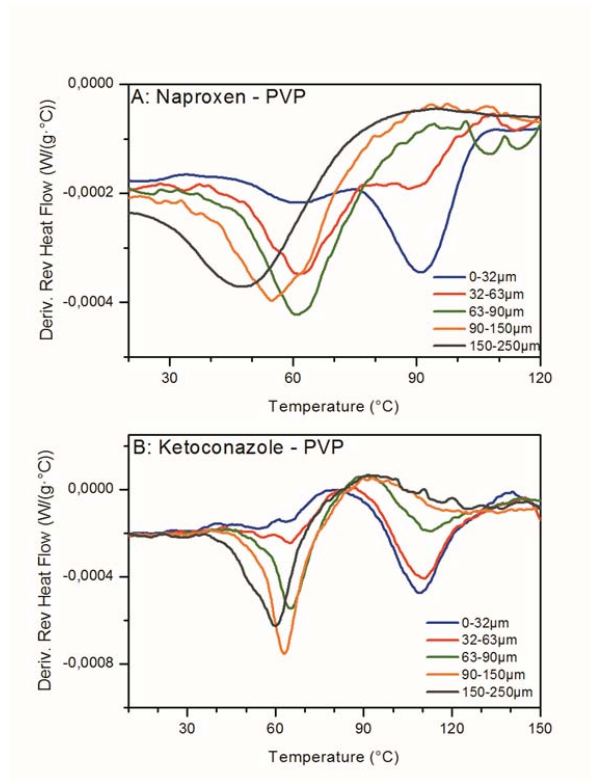


Figure 5: Derivative heat flow in function of temperature for the different particle size ranges of a INDO-PVP glass solution film, prepared from a DCM (A) and DCM-Methanol (B) solution.

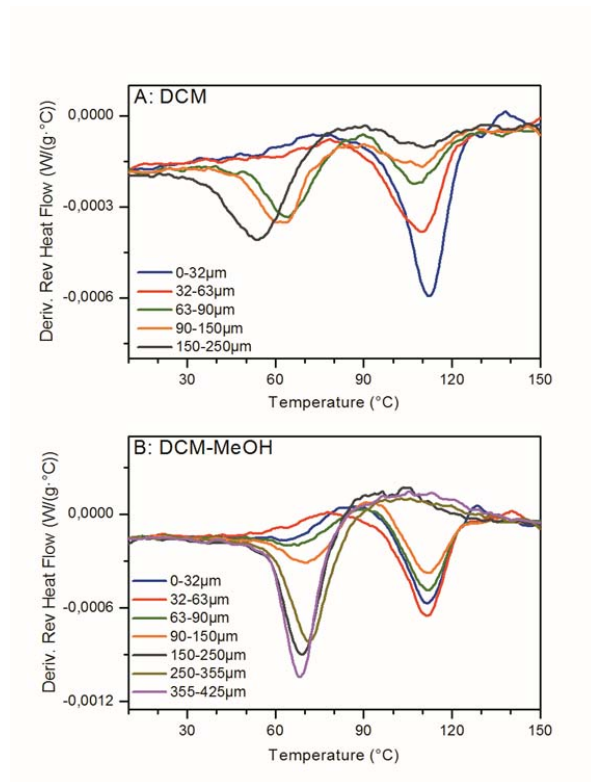


Figure 6: Weight (% , green line) and temperature (°C, blue line)in function of time (min) for INDO-PVP film particles with a size range of 0-32 $\mu\text{m}$ , 90-150 $\mu\text{m}$  and 250-355 $\mu\text{m}$ .

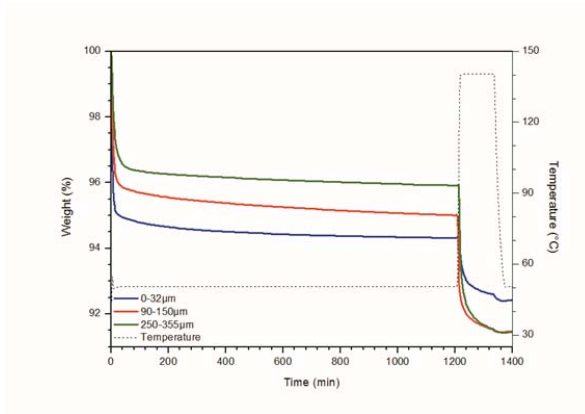


Figure 7: Depression on the Gordon-Taylor glass transition temperature in function of solvent loss from the glass transition to 170°C for all different particle size ranges, with trendline and R<sup>2</sup> value.

